Signal Processing 91 (2011) 988–999

Contents lists available at ScienceDirect

Signal Processing

journal homepage: www.elsevier.com/locate/sigpro

A novel fuzzy clustering algorithm with non local adaptive spatial constraint for image segmentation

Feng Zhao*, Licheng Jiao, Hanqiang Liu, Xinbo Gao

Key Laboratory of Intelligent Perception and Image Understanding of Ministry of Education of China, Institute of Intelligent Information Processing, Xidian University, Xi'an, PR China

ARTICLE INFO

Article history:
Received 1 February 2010
Received in revised form
17 September 2010
Accepted 1 October 2010
Available online 8 October 2010

Keywords:
Image segmentation
Fuzzy clustering algorithm
Non local spatial constraint
Adaptive spatial parameter
Magnetic resonance (MR) image

ABSTRACT

Generalized fuzzy *c*-means clustering algorithm with improved fuzzy partitions (GIFP_FCM) is a novel fuzzy clustering algorithm. However when GIFP_FCM is applied to image segmentation, it is sensitive to noise in the image because of ignoring the spatial information contained in the pixels. In order to solve this problem, a novel fuzzy clustering algorithm with non local adaptive spatial constraint (FCA_NLASC) is proposed in this paper. In the proposed method, a novel non local adaptive spatial constraint term is introduced to modify the objective function of GIFP_FCM. The characteristic of this technique is that the adaptive spatial parameter for each pixel is designed to make the non local spatial information of each pixel playing a different role in guiding the noisy image segmentation. Segmentation experiments on synthetic and real images, especially magnetic resonance (MR) images, are performed to assess the performance of an FCA_NLASC in comparison with GIFP_FCM and fuzzy *c*-means clustering algorithms with local spatial constraint. Experimental results show that the proposed method is robust to noise in the image and more effective than the comparative algorithms.

1. Introduction

Image segmentation is one of the most important research topics in computer vision and image understanding. The task of image segmentation is to partition an image into a number of non-overlapping regions with homogeneous characteristics, such as intensity, color, texture, etc. In the past few decades, many segmentation algorithms have been developed [1–5]. Fuzzy clustering is one of the most widely used techniques for image segmentation [5–8]. Due to introducing the fuzziness for the belongingness of each image pixel, fuzzy clustering can retain more information from the image than hard clustering. Fuzzy *c*-means clustering algorithm (FCM) [9] is the most popular fuzzy clustering algorithm and many newly proposed fuzzy clustering algorithms [10,11] originate from it. A main drawback of fuzzy clustering algorithms remains the sensitivity to noise in the image. In order to solve this problem, the local spatial information derived from the image is incorporated into the fuzzy clustering algorithms [12–15].

Generalized fuzzy *c*-means clustering algorithm with improved fuzzy partitions (GIFP_FCM) [11] is a novel fuzzy clustering algorithm. In GIFP_FCM, a new membership constraint term is introduced into the objective function of an FCM to force a more crisp partition. GIFP_FCM under an appropriate parameter α, which controls the convergence speed of GIFP_FCM, can converge more rapidly than an FCM. In [11], Zhu et al. claimed that GIFP_FCM behaves more robustly than an FCM in noisy texture image segmentation, when using Gabor filter to extract the texture feature. It is possible

* Corresponding author. Tel.: +86 029 8820 2661.
E-mail address: add_zf1119@hotmail.com (F. Zhao).

0165-1684/$ - see front matter © 2010 Elsevier B.V. All rights reserved.
doi:10.1016/j.sigpro.2010.10.001

that the robustness of GIFP_FCM is due to using Gabor texture features, which are complicated and of high-dimensional data. However, GIFP_FCM is still sensitive to noise, when it is applied to normal gray-level images. To be sure, the local spatial information derived from the image can be introduced into GIFP_FCM to overcome its sensitivity to noise in some degree. However, when the noise level in the image is high, the adjacent pixels of a pixel in the image may also contain an abnormal feature. Therefore, GIFP_FCM incorporating the local spatial information cannot obtain satisfying segmentation performance. In this paper, we first define a novel non local adaptive spatial constraint term using the non local spatial information, which is obtained by the non local mean strategy used in image restoration [16]. Then, we introduce this constraint term into the objective function of GIFP_FCM and propose a novel fuzzy clustering algorithm with non local adaptive spatial constraint (FCA_NLASC) to solve the sensitivity of GIFP_FCM to noise in gray images. In this algorithm, the adaptive spatial parameter for each pixel is designed to make the non local spatial information of each pixel playing a different part in guiding the noisy image segmentation. Due to utilizing the non local spatial information, FCA_NLASC is more effective than GIFP_FCM and fuzzy clustering algorithms, using the local spatial information in the noisy gray image segmentation.

The rest of this paper is organized as follows. Section 2 reviews fuzzy clustering algorithms. Fuzzy clustering algorithm with non local adaptive spatial constraint (FCA_NLASC) for image segmentation is proposed in Section 3. In Section 4, the parameters of FCA_NLASC are discussed and the segmentation experiments on synthetic and real images, especially MR images, are performed to verify the performance of an FCA_NLASC. Finally, some discussions and concluding remarks are given in Section 5.

2. Fuzzy clustering algorithms

Fuzzy c-means clustering algorithm (FCM) is one of the most widely used fuzzy clustering algorithms. Let $X=\{x_1, x_2, \ldots, x_n\}$ denote an image with n pixels, where x_j represents the gray value of the jth pixel. An FCM aims at partitioning X into c clusters by minimizing the following objective function

$$J_m = \sum_{i=1}^{c}\sum_{j=1}^{n} u_{ij}^m ||x_j - v_i||^2 \tag{1}$$

with the following constraints

$$\sum_{i=1}^{c} u_{ij} = 1, \quad u_{ij} \in [0, 1], \quad 0 \le \sum_{j=1}^{n} u_{ij} \le n, \tag{2}$$

where v_i denotes the center of the ith cluster, and u_{ij} represents the membership degree of the jth pixel belonging to the ith cluster. $||\ ||$ Denotes the Euclidean norm and the parameter m is a weighting exponent on each fuzzy membership that determines the amount of fuzziness of the resulting partition.

Generalized fuzzy c-means clustering algorithm with improved fuzzy partitions (GIFP_FCM) [11] is a novel modified version of an FCM. Through introducing a novel reward term for the membership of a single data point to force a more crisp assignment, GIFP_FCM with an appropriate parameter can converge more rapidly than an FCM. The objective function of GIFP_FCM is given as follows:

$$J_m = \sum_{i=1}^{c}\sum_{j=1}^{n} u_{ij}^m ||x_j - v_i||^2 + \sum_{j=1}^{n} a_j \sum_{i=1}^{c} u_{ij}(1-u_{ij}^{m-1}), \tag{3}$$

where the constraints in Eq. (2) must be satisfied. By minimizing Eq. (3) using Lagrange multiplier method, the update equations of membership function u_{ij} and cluster center v_i are presented as follows

$$u_{ij} = \frac{1}{\sum_{l=1}^{c} ((||x_j - v_i||^2 - a_j)/(||x_j - v_l||^2 - a_j))^{1/(m-1)}} \tag{4}$$

$$v_i = \frac{\sum_{j=1}^{n} u_{ij}^m x_j}{\sum_{j=1}^{n} u_{ij}^m}. \tag{5}$$

To make $0 \le u_{ij} \le 1$, $a_j = \alpha \min\{||x_j - v_t||^2 | t \in \{1, \ldots, c\}\}$, where the parameter $\alpha (0 < \alpha < 1)$ controls the convergence speed of GIFP_FCM.

3. Fuzzy clustering algorithm with non local adaptive spatial constraint (FCA_NLASC)

Due to not taking into account any spatial information in image context, GIFP_FCM is sensitive to noise in gray images. In order to overcome the sensitivity of GIFP_FCM to noise, the non local spatial information, which is obtained by the non local mean strategy used in image restoration [16], is incorporated into GIFP_FCM in this paper.

3.1. Non local spatial information

In order to make fuzzy clustering algorithms robust to noise in the image, the local spatial information derived from the image, such as the mean and median of neighboring pixels within a specified window around each pixel, is often incorporated into fuzzy clustering algorithms [12–15]. However, when the noise level in the image is high, the adjacent pixels of a pixel in the image may also contain an abnormal feature. In this condition, the local spatial information derived from the image cannot play a positive role in guiding the noisy image segmentation.

For every pixel in an image, there are a set of pixels with a similar neighborhood configuration of it [16]. Compared with only using the adjacent pixels of a pixel, it is more reasonable to utilize these similar pixels in the image to obtain the spatial information of the pixel. We call this kind of spatial information as the non local spatial information. In detail, for the jth pixel, its non local spatial information $\bar{x}_j$ can be computed by the following formula

$$\bar{x}_j = \sum_{p \in W_j^r} w_{jp} x_p, \tag{6}$$

where W_j^r denotes a search window of radius r and centered at the jth pixel, i.e., pixels in this domain are utilized to compute the spatial information of the jth pixel. The weights $w_{jp}(p \in W_j^r)$ rely on the similarity between the jth and pth pixels, and satisfy $0 \le w_{jp} \le 1$ and $\sum_{p \in W_j^r} w_{jp} = 1$. The similarity between the jth and pth pixels is computed by a weighted Euclidean distance $||x(N_j)-x(N_p)||_{2,\rho}^2$,[1] where $x(N_j)$ is the gray level vectors within the square neighborhood N_j of radius s and centered at the jth pixel. $||x(N_j)-x(N_p)||_{2,\rho}^2$ is defined as follows:

$$||x(N_j)-x(N_p)||_{2,\rho}^2 = \sum_{q=1}^{(2s+1)^2} \rho^{(q)}(x^{(q)}(N_j)-x^{(q)}(N_p))^2, \tag{7}$$

where $x^{(q)}(N_j)$ is the qth component of the vector $x(N_j)$ and $\rho^{(q)}$ is defined by

$$\rho^{(q)} = \sum_{t=\max(d,\,1)}^{s} \frac{1}{(2t+1)^2 s}, \quad d = \max(|y_q-s-1|,\, |z_q-s-1|), \tag{8}$$

where $y_q = \mathrm{mod}(q, (2s+1))$ and $z_q = floor(q, (2s+1))+1$. (y_q, z_q) denote the coordinates of the qth component in the square neighborhood window. Under a fixed s, $\rho^{(q)}$ can be computed in advance. Thus, the weight w_{jp} between the jth and pth pixels is defined as follows:

$$w_{jp} = \frac{1}{Z_j} \exp\left(-||x(N_j)-x(N_p)||_{2,\rho}^2/h\right), \tag{9}$$

where h is the filtering degree parameter, which controls the decay of the weight function w_{jp}, and Z_j is the normalizing constant defined as

$$Z_j = \sum_{p \in W_j^r} \exp\left(-||x(N_j)-x(N_p)||_{2,\rho}^2/h\right).$$

Therefore, the pixels with a similar gray level neighborhood to $x(N_j)$ own larger weights.

Actually, the larger the radius of search window r is, the more the number of the pixels having the similar neighborhood configuration is. When we utilize more pixels with the similar neighborhood configuration of the jth pixel to compute its spatial information, the obtained spatial information $\bar{x}_j$ is more effective. In theory, the spatial information $\bar{x}_j$ can be computed as the weighted average of all the pixels in the image. Due to considering the computational complexity, the r value cannot be set too large. In the experimental section, we discuss the parameter r and give its reference value. In contrast, traditional local methods [12–15] cannot utilize the neighborhood window with a large radius to compute the spatial information, due to the results under large neighborhood windows heavily suffering from the blurring problem. In a word, our proposed spatial information can consider the larger range around the pixel, while utilizes the neighborhood configuration of the pixels in the image. In order to distinguish this spatial information and the traditional local spatial information, we call this kind of spatial information as non-local spatial information.

[1] http://www.mathworks.com/matlabcentral/fileexchange/13176-non-local-means-filter.

3.2. Design of objective function and adaptive spatial parameter in FCA_NLASC

In this paper, we utilize the non local spatial information derived from the image to define a novel non local adaptive spatial constraint term $\sum_{i=1}^{c}\sum_{j=1}^{n} \beta_j u_{ij}^m \times ||\bar{x}_j - v_i||^2$, where $\bar{x}_j$ is the non local spatial information of the jth pixel, and β_j is the adaptive spatial parameter which controls the penalty effect of the spatial constraint of the jth pixel. Then, we introduce this constraint term into the objective function of GIFP_FCM and propose a fuzzy clustering algorithm with non local adaptive spatial constraint (FCA_NLASC). The objective function of an FCA_NLASC is presented as follows

$$J_m = \sum_{i=1}^{c}\sum_{j=1}^{n} u_{ij}^m ||x_j - v_i||^2 + \sum_{i=1}^{c}\sum_{j=1}^{n} [a_j u_{ij}(1-u_{ij}^{m-1}) + \beta_j u_{ij}^m ||\bar{x}_j - v_i||^2], \tag{10}$$

where the constraints in Eq. (2) must be satisfied.

By minimizing Eq. (10) using the Lagrange multiplier method, the update equations of membership function u_{ij} and the cluster center v_i are given in Eqs. (11) and (12), and the details of proving process are presented in Appendix.

$$u_{ij} = \frac{1}{\sum_{l=1}^{c}\left(\frac{||x_j - v_i||^2 - a_j + \beta_j||\bar{x}_j - v_i||^2}{||x_j - v_l||^2 - a_j + \beta_j||\bar{x}_j - v_l||^2}\right)^{1/(m-1)}} \tag{11}$$

$$v_i = \frac{\sum_{j=1}^{n} u_{ij}^m (x_j + \beta_j \bar{x}_j)}{\sum_{j=1}^{n}(1+\beta_j)u_{ij}^m}. \tag{12}$$

In order to make $0 \le u_{ij} \le 1$, we define $a_j = \alpha \min\{||x_j - v_t||^2 + \beta_j ||\bar{x}_j - v_t||^2 | t \in \{1,\ldots,c\}\}$, $(0 < \alpha < 1)$ in this paper. How to set the parameter α is given in the experimental section. Furthermore, the design of parameter β_j is introduced in the following paragraph.

In an FCA_NLASC, we utilize the weights $w_{jp}(p \in W_j^r)$ to determine the adaptive spatial parameter β_j for the jth pixel $(1 \le j \le n)$. Intuitively, it would be better if we can adjust the spatial constraint separately for each pixel, i.e., the jth pixel possesses its own β_j value. The parameter β_j is defined as

$$\beta_j = \beta_{\min} + (\beta_{\max} - \beta_{\min}) \frac{\delta_j - \min\limits_{1 \le l \le n}\{\delta_l\}}{\max\limits_{1 \le l \le n}\{\delta_l\} - \min\limits_{1 \le l \le n}\{\delta_l\}}, \tag{13}$$

where $[\beta_{\min}, \beta_{\max}]$ denotes the range of β_j, and $\delta_j = \max\limits_{p \in W_j^r}(w_{jp})$ is the maximum weight of pixels in the window W_j^r centered at the jth pixel. The value of δ_j $(1 \le j \le n)$ can reflect the accuracy of $\bar{x}_j$, estimating for the jth pixel value of the original image (non noisy image) in some degree. Thus, the larger the δ_j is, the bigger the spatial constraint effect of $\bar{x}_j$ on x_j is. Therefore, β_j obtained

by Eq. (13) can make the non local spatial constraint of each pixel able to play a different part in guiding the noisy image segmentation. The parameters $\beta_{\min}$ and $\beta_{\max}$ are analyzed in the experimental section.

Then, we adopt a noise-corrupted image as an example to show the effect of the non local adaptive spatial constraint term. Two image blocks A and B are extracted from the image and shown in the left part of Fig. 1. For the

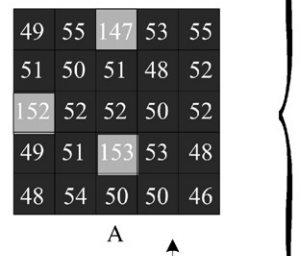

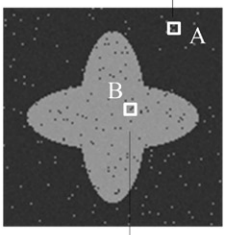

The initial membership values of the image block A

0.78731	0.21239	0.46977	0.35897	0.65685
0.46521	0.54646	0.37337	0.74624	0.8927
0.97763	0.3657	0.76937	0.31184	0.76175
0.43856	0.58103	0.53972	0.92858	0.15206
0.65663	0.23034	0.63266	0.09367	0.31946

The final membership values obtained by GIFP_FCM

1	0.99997	9.8301e-006	0.99999	0.99997
1	1	1	1	1
3.6932e-006	1	1	1	1
1	1	8.264e-006	0.99999	1
1	0.99998	1	1	0.99999

The final membership values obtained by FCA_NLASC

1	1	0.99907	1	1
1	1	1	1	1
0.99894	1	1	1	1
1	1	0.99891	1	1
1	1	1	1	1

The initial membership values of the image block B

0.36687	0.62543	0.73055	0.26637	0.36537
0.47596	0.89194	0.87066	0.38138	0.46985
0.38649	0.49734	0.70716	0.79576	0.17501
0.946	0.57893	0.36592	0.66151	0.51028
0.7793	0.39708	0.46678	0.68373	0.14518

The final membership values obtained by GIFP_FCM

1.6009e-009	1.6009e-009	8.264e-006	1.1035e-006	9.8301e-006
1.6009e-009	1.6009e-009	1.1035e-006	1	9.0336e-007
8.264e-006	9.0336e-007	1	3.6932e-006	9.8301e-006
1.1035e-006	1.7738e-005	9.8301e-006	9.8301e-006	3.6932e-006
1.1035e-006	4.3344e-006	1.7738e-005	2.8219e-005	1.1035e-006

The final membership values obtained by FCA_NLASC

1.6531e-006	1.2945e-006	3.0107e-006	5.9464e-007	5.3021e-007
1.6262e-006	1.4754e-006	7.0223e-007	0.00094674	1.676e-006
3.3419e-006	1.8313e-006	0.00097269	2.0123e-006	8.4783e-007
8.0623e-007	5.2928e-007	3.2648e-007	4.3972e-007	1.905e-006
8.0746e-007	5.2077e-007	8.6255e-007	1.1845e-006	9.7768e-007

Fig. 1. Effect of the non local adaptive spatial constraint terms: A and B are 5×5 image blocks with noise (marked with a rectangle in the image) and the right column shows their corresponding initial membership values and final membership values obtained by GIFP_FCM and FCA_NLASC.

image block A, the central pixel is not corrupted by noise and there are three noisy pixels within this block. For the image block B, the central pixel and one neighboring pixel are corrupted by noise. Furthermore, the initial membership values and the final membership values obtained by GIFP_FCM and FCA_NLASC on these two image blocks are illustrated in the right part of Fig. 1. It can be found from Fig. 1 that the final membership values obtained by GIFP_FCM for these noisy pixels are far different from the membership values of the other non noisy pixels within the block. Thus, GIFP_FCM cannot correctly classify these noisy pixels in the image blocks A and B. In contrast, it is clearly shown that the final membership values obtained by an FCA_NLASC for these noisy pixels are very similar to the membership values of the other non noisy pixels within the block. Thus, FCA_NLASC can correctly classify the noisy pixels in the image blocks A and B. In a word, the introduction of the non local adaptive spatial constraint term suppresses the influence of noise and makes an FCA_NLASC robust to noise in the image.

3.3. Description of the proposed FCA_NLASC

The details of fuzzy clustering algorithm with non local adaptive spatial constraint (FCA_NLASC) for image segmentation are described as follows.

Input: image $X=\{x_1, x_2, \ldots, x_n\}$, the number of clusters c $(2 \le c \le n)$, the threshold ε, the maximum number of iterations T, the radius of search window r, the radius of square neighborhood s and the filtering degree parameter h.

Output: segmentation result of X.

Step 1: initialize the cluster centers $V^{(1)} = [v_1^{(1)}, v_2^{(1)}, \ldots, v_c^{(1)}]$ and set the iterative index $k=1$.

Step 2: obtain the non local spatial information of each pixel. In detail, firstly compute the weighted Euclidean distance $||x(N_j)-x(N_p)||_{2,\rho}^2$ using Eq. (7), then compute the weight w_{jp} using Eq. (9), eventually obtain the non local spatial information $\bar{x}_j$ for the jth pixel $(1 \le j \le n)$ using Eq. (6).

Step 3: compute the adaptive spatial parameter β_j for the jth pixel $(1 \le j \le n)$ using Eq. (13).

Step 4: update the membership functions $u_{ij}^{(k)}$ using Eq. (11).

Step 5: compute the cluster centers $v_i^{(k+1)}$ using Eq. (12).

Step 6: if $||V^{(k+1)}-V^{(k)}|| < \varepsilon$ or the number of iterations $k > T$, then output the segmentation result, otherwise $k=k+1$, go to Step 4.

4. Experimental results and analysis

In this section, we perform experiments on synthetic and real images, especially MR images, to demonstrate the performance of an FCA_NLASC. We take GIFP_FCM [11], FCM_S1 [13] and FCM_S2 [13] as comparative methods. For FCM_S1 and FCM_S2, the mean and median of the neighbors within a 3×3 window around each pixel in the image are taken as the local information of the pixel, respectively. For these four methods, the fuzziness index m, the maximal iteration num$T$ and the threshold ε are set to 2500 and 10^{-5}, respectively. Furthermore, the effect of the parameter α on the algorithm performance of GIFP_FCM was discussed in [11] in detail. It can be found from the experimental results presented in [11] that GIFP_FCM can obtain satisfying clustering performance and fast convergence speed when $\alpha \ge 0.9$. Therefore, the parameter α for GIFP_FCM and FCA_NLASC in our experiments is set to 0.99.

4.1. Experiment on synthetic image

4.1.1. Analysis of the adaptive spatial parameter

A synthetic image containing 256×256 pixels is presented in Fig. 2(a). The image includes four clusters with the corresponding gray values taken as 0, 85, 170 and 255. In all the experiments, we adopt function imnoise in matlab to add Gaussian noise to images. In this section, we, respectively, add Gaussian noise of mean 0 and variance 0.006, 0.016 and 0.026 to this image, shown in Fig. 2(b)–(d). As presented in Eq. (13), the adaptive spatial parameter β_j of the jth pixel is related to $\beta_{\min}$ and $\beta_{\max}$. It can be found from Eqs. (10) and (13) that too small $\beta_{\min}$ and $\beta_{\max}$ may make the spatial constraints of some pixels unable to guide the pixel clustering, and too large $\beta_{\max}$ may lead to the pixel clustering heavily relying on the spatial constraint. In [13], the spatial parameter β of FCM_S1 and FCM_S2 was verified in the interval $(0, 8)$. In this experiment, we set $\beta_{\max}=12$ and test $\beta_{\min}$ on the set $[0.3, 0.6, \ldots, 12]$ to make β_j vary in the interval $(0, 12)$. We use these three noisy images shown in Fig. 2(b)–(d) as the test images to verify the effect of $\beta_{\min}$ on the performance of an FCA_NLASC. The clustering accuracy (CA) [17] is adopted to evaluate the algorithm performance. Here, the radius of search window r, the radius of square neighborhood s and the filtering degree parameter h are set to 10, 3 and 800, respectively. We perform 10 independent runs of an FCA_NLASC under each $\beta_{\min}$ value and present the average CA curves on these three noisy images in Fig. 2(e)–(g).

It was pointed out in [13] that the spatial parameter β in FCM_S1 and FCM_S2 can affect the clustering results. In order to make a fair comparison with an FCA_NLASC, the parameter β for FCM_S1 and FCM_S2 varies from 0.3 to 12 with the increment 0.3. We still perform 10 independent runs of these two methods under each β value and show the average CA curves on these three noisy images in Fig. 2(e)–(g). For these three noisy images, an FCA_NLASC outperforms FCM_S1 and FCM_S2 under all the $\beta_{\min}$ (β) values. As shown in Fig. 2(e) and (f), when the noise level in the image is not high, CA values of FCA_NLASC with the increase of $\beta_{\min}$ almost remain constant. However, as shown in Fig. 2(g), the $\beta_{\min}$ value has a certain effect on the performance of FCA_NLASC, when the noise level in the image is high. In detail, CA of FCA_NLASC increases with $\beta_{\min}$ and presents no apparent changes after $\beta_{\min}=6$. Therefore, when the noise level in the image is high, one can properly increase the $\beta_{\min}$ value to improve the algorithm performance of an FCA_NLASC.

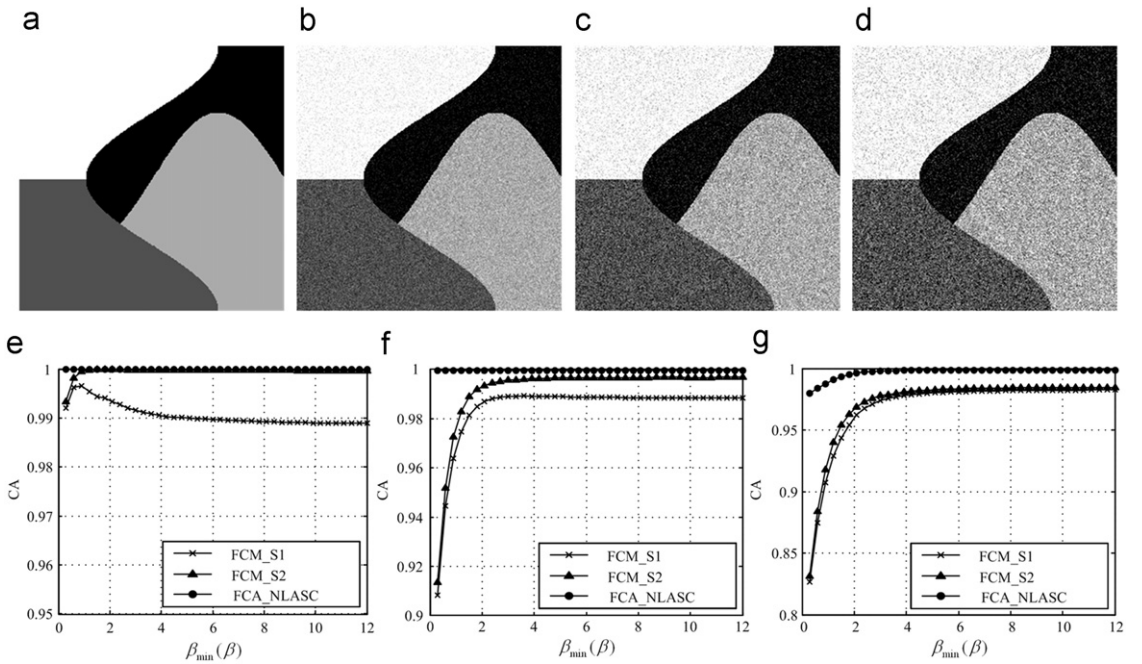

Fig. 2. CA of FCA_NLASC (FCM_S1 and FCM_S1) against $\beta_{\min}(\beta)$: (a) original image; (b) noisy image with Gaussian noise (0, 0.006); (c) noisy image with Gaussian noise (0, 0.016); (d) noisy image with Gaussian noise (0, 0.026); (e) CA versus $\beta_{\min}(\beta)$ on (b); (f) CA versus $\beta_{\min}(\beta)$ on (c); and (g) CA versus $\beta_{\min}(\beta)$ on (d).

4.1.2. *Analysis of the non local spatial information parameters*

The radius of search window r, the radius of square neighborhood s and the filtering degree parameter h are related to the non local spatial information of the pixels in the image. How to set these three parameters is still an open problem.

Especially, the parameter h controls the decay of the weight function in Eq. (9) and can greatly influence the quality of the non local spatial information. Here, we set $\beta_{\min}=6$, $\beta_{\max}=12$, $r=10$ and $s=3$, and test h on the set [50, 100, …, 1200]. Actually, the parameter h should be set according to the noise level in the image. In this experiment, we add Gaussian noise of mean 0 and variance varying from 0.002 to 0.03 with the increment 0.002 to the synthetic image (as shown in Fig. 2(a)) to generate the noisy images with different noise level. The average CA value of 10 runs of an FCA_NLASC under each (h, *noise level*) pair is presented in Fig. 3. It reveals that the parameter h has a certain influence on the performance of FCA_NLASC, and FCA_NLASC under small h value cannot obtain satisfying segmentation performance, when the noise level in the image is high. Thus, the parameter h should increase with the noise level of the image in order to achieve satisfying performance. Then, we extract CA curves of FCA_NLASC on the images with Gaussian noise (0, 0.006), (0, 0.016) and (0, 0.026) from Fig. 3, and show them in Fig. 4(a)–(c), respectively. For the image with Gaussian noise (0, 0.006), CA first presents a short increase with h and achieves the maximum value at $h=250$, then decreases with h within a small descending range (less than 0.05%). For the image with Gaussian noise

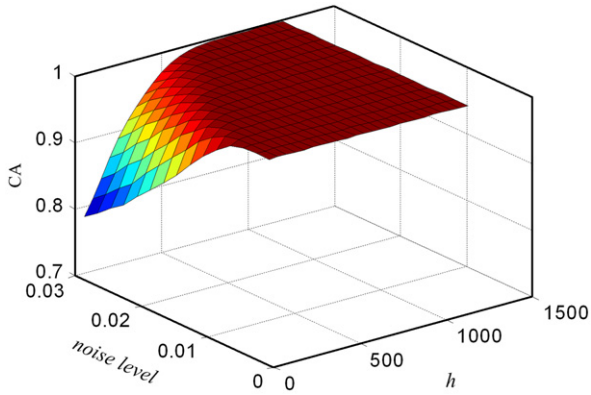

Fig. 3. CA of FCA_NLASC versus the filtering degree parameter h and the noise level.

(0, 0.016), CA first shows a sharp increase with h and achieves the maximum value at $h=750$, then slowly decreases with h (the descending range less than 0.02%). For the image with Gaussian noise (0, 0.026), CA increases with h and achieves the maximum value at $h=950$, then presents no apparent changes ($<0.006\%$). It is found from these three curves that $h=800$ may be a suitable value, when an FCA_NLASC is applied to noisy image segmentation.

Then, we evaluate the effect of the search window radius r and the square neighborhood radius s on the performance of an FCA_NLASC. Here, we set $\beta_{\min}=6$, $\beta_{\max}=12$ and $h=800$, and test r and s on the sets [4, 6, …, 12] and [1, 2, …, 6], respectively. In this experiment,

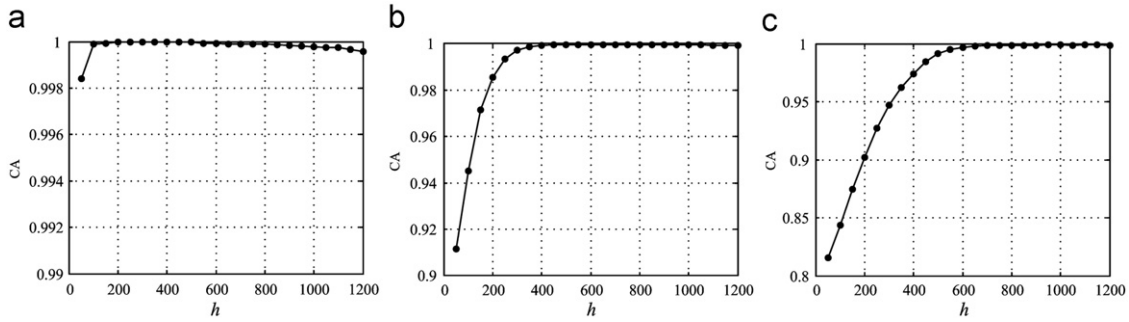

Fig. 4. CA of FCA_NLASC versus the filtering degree parameter h: (a) curve on the image with Gaussian noise (0, 0.006); (b) curve on the image with Gaussian noise (0, 0.016) and (c) curve on the image with Gaussian noise (0, 0.026).

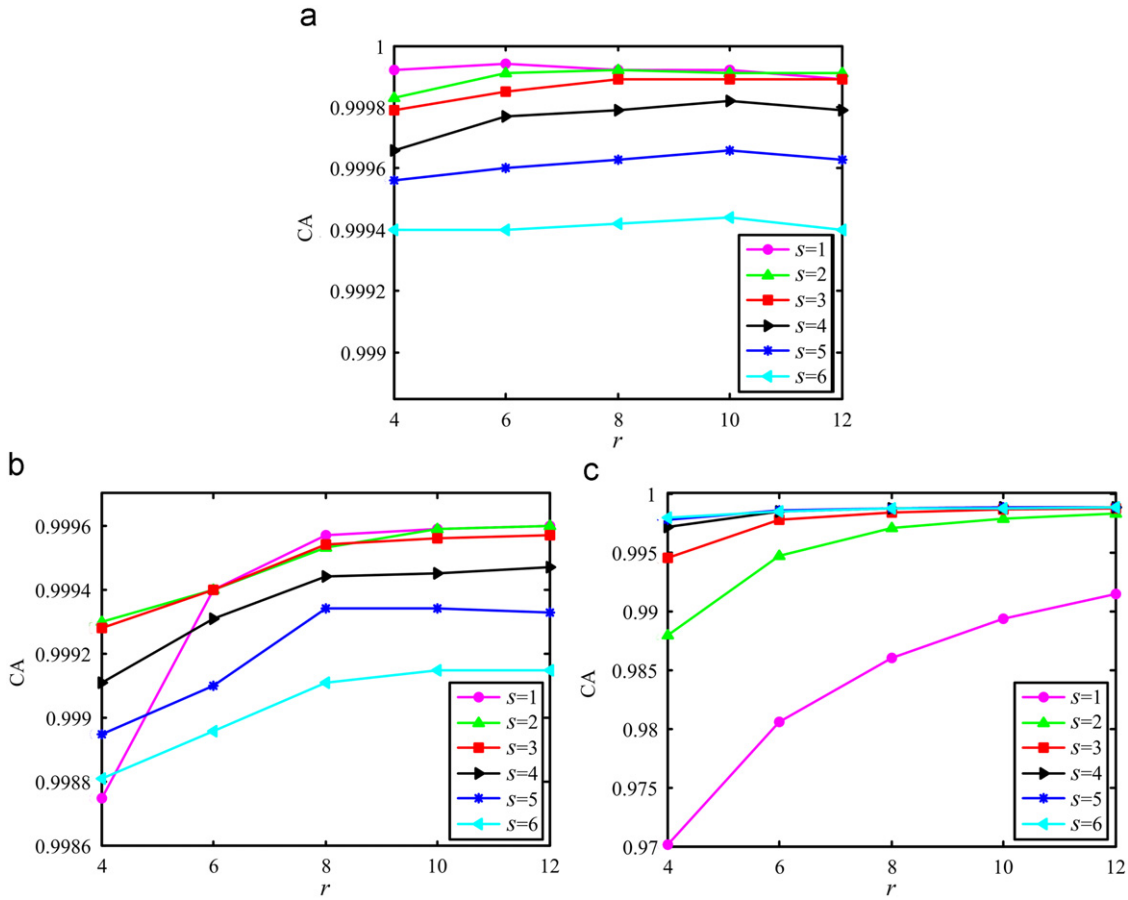

Fig. 5. CA of FCA_NLASC under different search window radius r and square neighborhood radius s: (a) curves on the image with Gaussian noise (0, 0.006); (b) curves on the image with Gaussian noise (0, 0.016); (c) curves on the image with Gaussian noise (0, 0.026).

we adopt these three noisy images shown in Fig. 2(b)–(d) as the test images and perform 10 independent runs of FCA_NLASC under each pair (r, s). Under each s value, the average CA curve of an FCA_NLASC with the increase of r value is shown in Fig. 5. It can be found from Fig. 5(a) to (c) that an FCA_NLASC under $s=3$ can obtain satisfying performance on these three noisy images. As shown in Fig. 5(a), the parameter r has no obvious influence on the algorithm performance, when the noise level in the image is low. In contrast, as shown in Fig. 5(b) and (c), the algorithm performance can be improved with the increase of r value in most cases, when FCA_NLASC is applied to the noisy images with Gaussian noise (0, 0.016) and (0, 0.026), respectively. Furthermore, the complexity of computing the non local spatial information for each pixel is $O((2r+1)^2(2s+1)^2)$, so it is not reasonable to assign too large values to the parameters r and s. Except the CA curve under $s=1$ shown in Fig. 5(c), the algorithm performance

under $r=10$ is satisfying. Therefore, $r=10$ and $s=3$ may be the suitable values for an FCA_NLASC.

4.1.3. Segmentation results of the synthetic image

Furthermore, we take the noisy image with Gaussian noise (0, 0.026), shown in Fig. 2(d), as an example to show the segmentation results of GIFP_FCM, FCM_S1, FCM_S2 and FCA_NLASC. In this experiment, we set $\beta_{\min}=6$, $\beta_{\max}=12$, $r=10$, $s=3$ and $h=800$ for FCA_NLASC according to the parameter analysis in the last two sections. In order to make a fair comparison with FCM_S1 and FCM_S2, we perform these two methods under $\beta=6$ and $\beta=12$. The segmentation results of these four methods on this noisy image are shown in Fig. 6. It is found from these results that FCA_NLASC can achieve more satisfying segmentation performance than GIFP_FCM, FCM_S1 and FCM_S2, which is also verified by the CA values of these methods.

4.2. Experiment on real image

Figs. 7(a) and 8(a) present two real images, the House image with 256×256 pixels and the Source image with 272×265 pixels. We add Gaussian noise (0, 0.006) and (0, 0.025) to these two images, respectively, and show the noisy images in Figs. 7(b) and 8(b). In this section, we adopt these two noisy images to testify the performance of GIFP_FCM, FCM_S1, FCM_S2 and FCA_NLASC. The segmentation results on these two noisy images are shown in Figs. 7(c)–(h) and 8(c)–(h), respectively. In this experiment, we set $\beta_{\min}=6$, $\beta_{\max}=12$, $r=10$, $s=3$ and $h=800$ for an FCA_NLASC according to the parameter analysis in Section 4.1. Furthermore, we perform FCM_S1 and FCM_S2 under $\beta=6$ and $\beta=12$. It is found from Figs. 7 and 8 that an FCA_NLASC can obtain better segmentation performance than GIFP_FCM, FCM_S1 and FCM_S2 on Gaussian noisy images. In order to quantitatively assess these four methods, the partition coefficient V_{pc} [18] and the partition entropy V_{pe} [19] are adopted to evaluate the segmentation results. The partition coefficient V_{pc} and the partition entropy V_{pe} are two cluster validity functions, which are defined as follows:

$$V_{\mathrm{pc}}=\sum_{i=1}^{c}\sum_{j=1}^{n}u_{ij}^{2}/n \tag{14}$$

$$V_{\mathrm{pe}}=-\sum_{i=1}^{c}\sum_{j=1}^{n}(u_{ij}\log u_{ij})/n. \tag{15}$$

The idea of these two validity functions is that the partition with less fuzziness means better performance. So the best clustering is achieved when V_{pc} is maximal and V_{pe} is minimal. The V_{pc} and V_{pe} values of these four

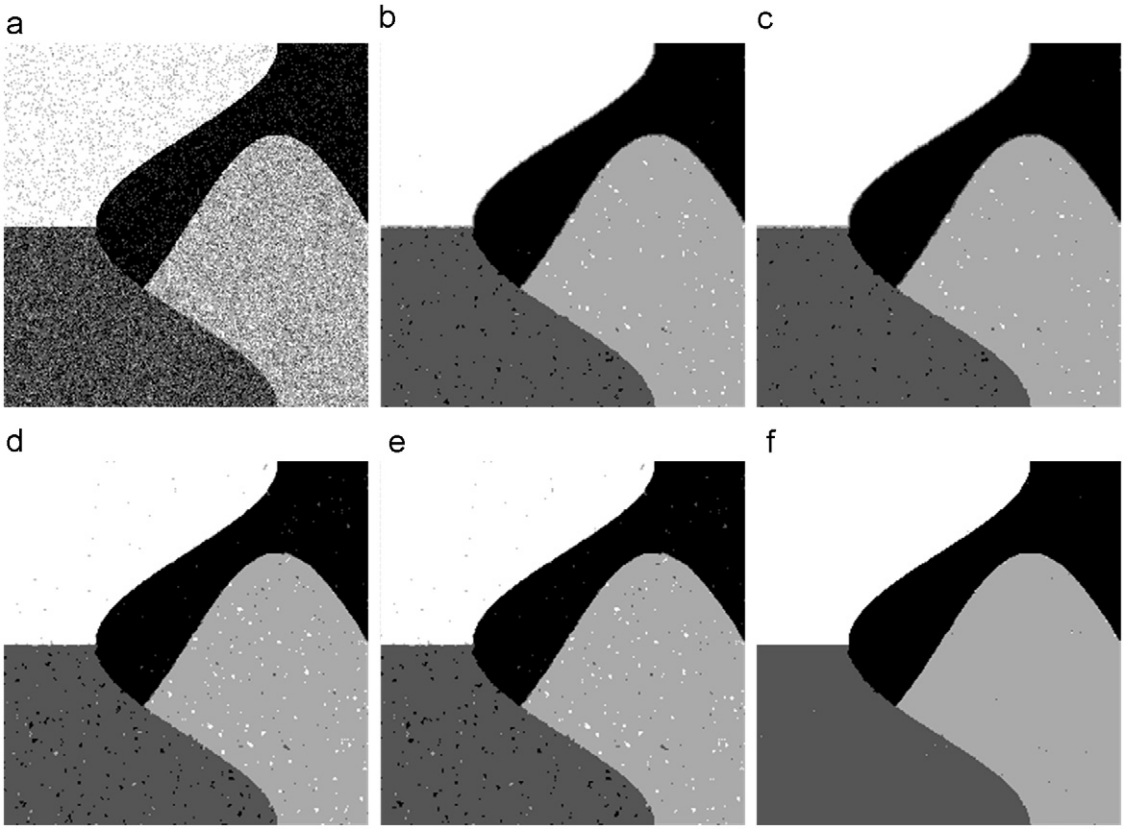

Fig. 6. Segmentation results on the synthetic image corrupted by Gaussian noise (0, 0.026): (a) GIFP_FCM result (CA=0.7511); (b) FCM_S1 result ($\beta=6$, CA=0.9810); (c) FCM_S1 result ($\beta=12$, CA=0.9826); (d) FCM_S2 result ($\beta=6$, CA=0.9835); (e) FCM_S2 result ($\beta=12$, CA=0.9846) and (f) FCA_NLASC result (CA=0.9986).

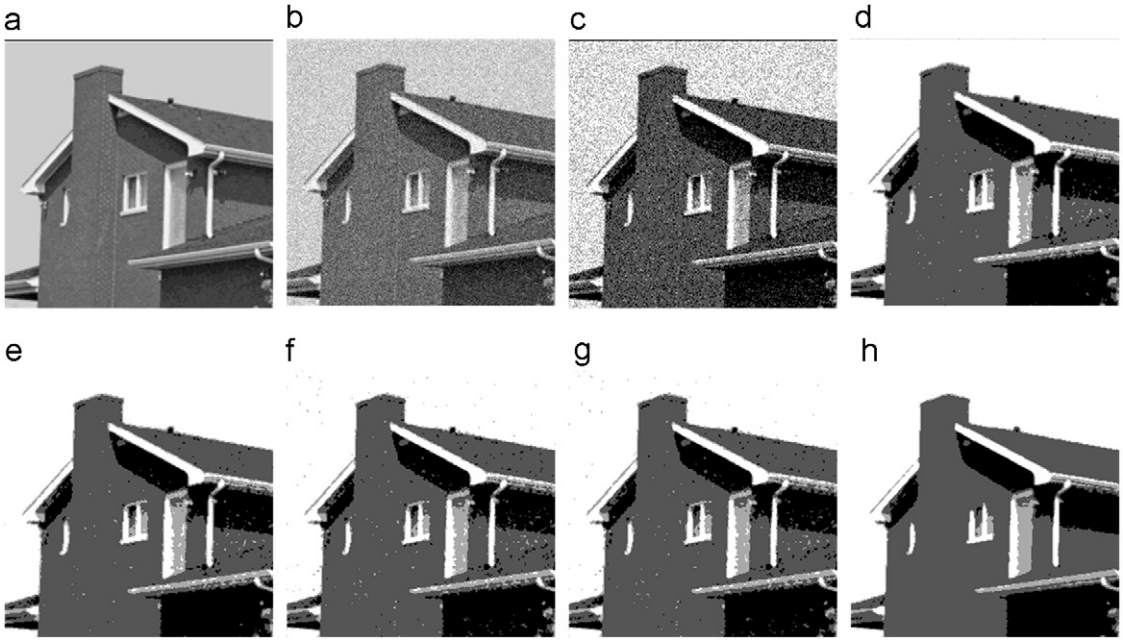

Fig. 7. Segmentation results on the House image corrupted by Gaussian noise: (a) original image; (b) noisy image; (c) GIFP_FCM result; (d) FCM_S1 result (β=6); (e) FCM_S1 result (β=12); (f) FCM_S2 result (β=6); (g) FCM_S2 result (β=12) and (h) FCA_NLASC result.

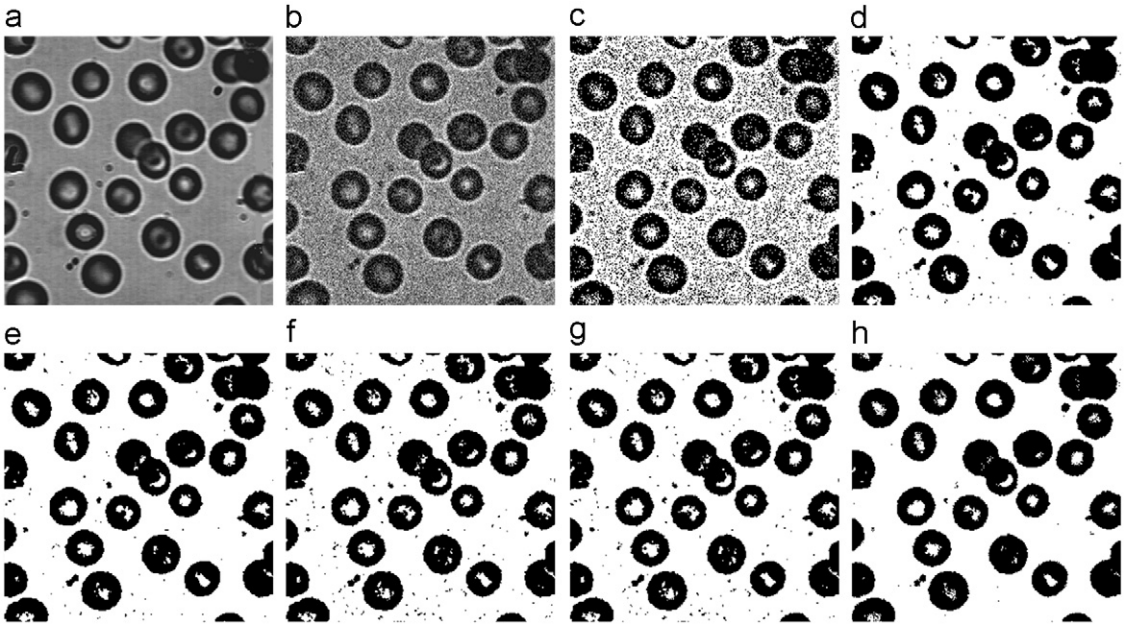

Fig. 8. Segmentation results on the Source image corrupted by Gaussian noise: (a) original image; (b) noisy image; (c) GIFP_FCM result; (d) FCM_S1 result (β=6); (e) FCM_S1 result (β=12); (f) FCM_S2 result (β=6); (g) FCM_S2 result (β=12) and (h) FCA_NLASC result.

methods on these two noisy images are presented in Table 1. As pointed out in Section 2, GIFP_FCM introduces the membership constraint term into the objective function of an FCM to force a more crisp partition. Therefore, it is normal for GIFP_FCM to obtain much higher V_{pc} and much lower V_{pe} values than FCM_S1 and FCM_S2, as shown in Table 1. What is more important, an FCA_NLASC achieves higher V_{pc} and lower V_{pe} values than GIFP_FCM. It reveals that an FCA_NLASC is more effective than GIFP_FCM in noisy image segmentation.

4.3. Experiment on an MR image

In this section, two MR images, MR1 and MR2, are adopted to test the performance of GIFP_FCM, FCM_S1,

Table 1
Comparison of these four methods on two real images corrupted by Gaussian noise.

		GIFP_FCM	FCM_S1		FCM_S2		FCA_NLASC
			β=6	β=12	β=6	β=12	
House	V_{pc}	0.9862	0.8165	0.8360	0.8071	0.8237	**0.9957**
	V_{pe}	0.0341	0.3754	0.3388	0.3906	0.3594	**0.0120**
Source	V_{pc}	0.9898	0.8808	0.8932	0.8745	0.8852	**0.9965**
	V_{pe}	0.0234	0.2145	0.1944	0.2232	0.2059	**0.0091**

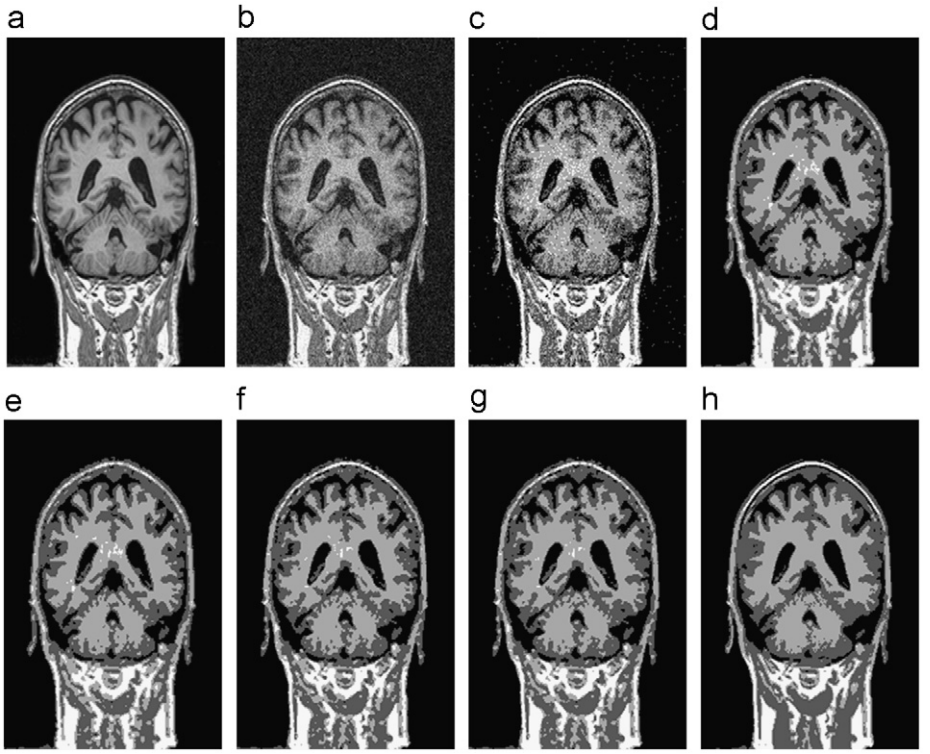

Fig. 9. Segmentation results on the MR1 image corrupted by Rician noise: (a) original image; (b) noisy image; (c) GIFP_FCM result; (d) FCM_S1 result (β=6); (e) FCM_S1 result (β=12); (f) FCM_S2 result (β=6); (g) FCM_S2 result (β=12) and (h) FCA_NLASC result.

FCM_S2 and FCA_NLASC. They are with 256×170 and 256×256 pixels, respectively, and shown in Figs. 9(a) and 10(a). It is known that MR images are always contaminated by Rician noise. Therefore, we add Rician noise of noise level (I=20) to these two images, shown in Figs. 9(b) and 10(b). In this experiment, Rician noise is generated by a code obtained from Ged Ridgway.[2] The segmentation results on these two Rician noisy MR images are presented in Figs. 9(c)–(h) and 10(c)–(h). The parameter setting for these four methods in this experiment is the same to that of Section 4.2. These segmentation results reveal that FCA_NLASC can effectively remove the noise and retain the edges in the MR images well. The V_{pc} and V_{pe} values of these four methods on these two noisy images are recorded in Table 2. It shows that an FCA_NLASC obtains the maximum V_{pc} and minimum V_{pe} values among these four methods.

5. Conclusion

In order to overcome the sensitivity of GIFP_FCM to noise in gray images, a novel fuzzy clustering algorithm with non local adaptive spatial constraint (FCA_NLASC) is proposed in this paper. This method utilizes the non local spatial information of each pixel in the image to guide the noisy image segmentation. The experimental results show that an FCA_NLASC can obtain satisfying segmentation performance on noisy images. In this paper, some parameters of an FCA_NLASC are preliminarily discussed in the experiment section. Thus, how to theoretically choose these parameters deserves to be studied. Furthermore, our further works also include utilizing the non

[2] http://www.mathworks.com/matlabcentral/fileexchange/14237.

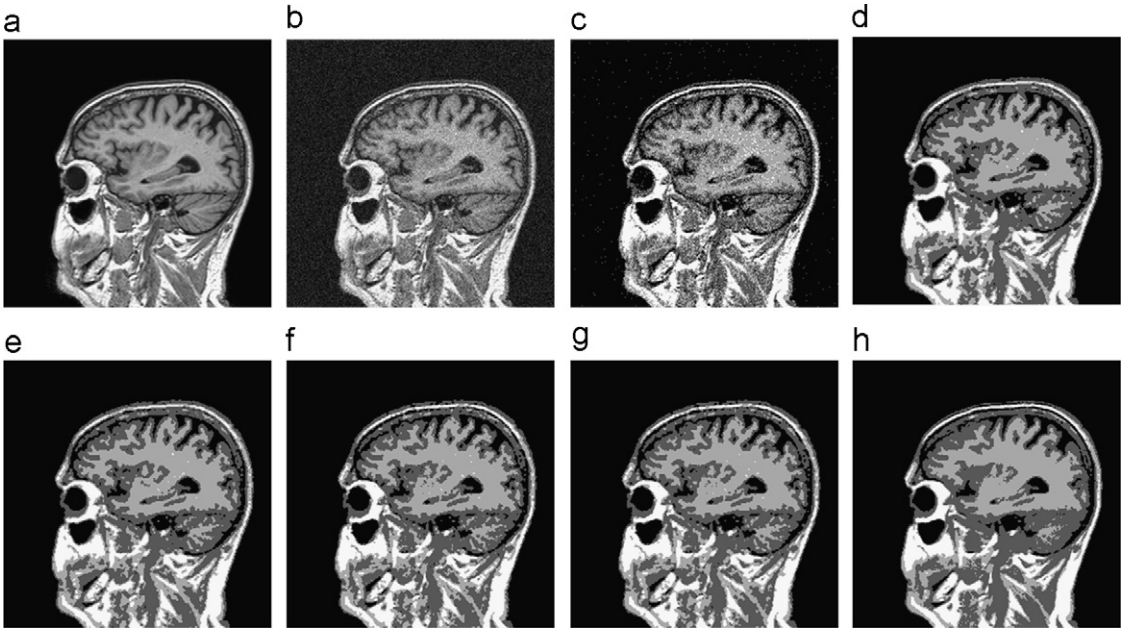

Fig. 10. Segmentation results on the MR2 image corrupted by Rician noise: (a) original image; (b) noisy image; (c) GIFP_FCM result; (d) FCM_S1 result (β=6); (e) FCM_S1 result (β=12); (f) FCM_S2 result (β=6); (g) FCM_S2 result (β=12) and (h) FCA_NLASC result.

Table 2
Comparison of these four methods on two MR images corrupted by Rician noise.

		GIFP_FCM	FCM_S1		FCM_S2		FCA_NLASC
			β=6	β=12	β=6	β=12	
MR1	V_{pc}	0.9897	0.8220	0.8318	0.8306	0.8388	**0.9913**
	V_{pe}	0.0252	0.3490	0.3296	0.3337	0.3172	**0.0214**
MR2	V_{pc}	0.9903	0.8345	0.8429	0.8393	0.8469	**0.9911**
	V_{pe}	0.0239	0.3259	0.3086	0.3179	0.3024	**0.0217**

local spatial information of the image to adaptively determine the clustering number in our method.

Acknowledgments

The authors would like to thank the anonymous reviewers for their detailed review and constructive comments. This work is supported by the National Natural Science Foundation of China (Grant nos. 60702062 and 60970067), the National High Technology Research and Development Program (863 Program) of China (Grant nos. 2008AA01Z125 and 2009AA12Z210), and the Fund for Foreign Scholars in University Research and Teaching Programs (the 111 Project) (Grant no. B07048).

Appendix

Theorem. The necessary condition for the minimization of the objective function in Eq. (10) with the constraints in Eq. (2) yields the following membership function and cluster center update equations

$$u_{ij}=\frac{1}{\sum_{l=1}^{c}\left(\frac{||x_j-v_i||^2-a_j+\beta_j||\bar{x}_j-v_i||^2}{||x_j-v_l||^2-a_j+\beta_j||\bar{x}_j-v_l||^2}\right)^{1/(m-1)}}$$

$$v_i=\frac{\sum_{j=1}^{n}u_{ij}^m(x_j+\beta_j\bar{x}_j)}{\sum_{j=1}^{n}(1+\beta_j)u_{ij}^m}.$$

Proof. According to the Lagrange multiplier method, the minimization of Eq. (10) can be transformed into the following unconstrained minimization problem:

$$\begin{aligned}L(u_{ij},v_i,\lambda_j,a_j,\beta_j)=&\sum_{i=1}^{c}\sum_{j=1}^{n}u_{ij}^m||x_j-v_i||^2\\&+\sum_{i=1}^{c}\sum_{j=1}^{n}[a_ju_{ij}(1-u_{ij}^{m-1})+\beta_ju_{ij}^m||\bar{x}_j-v_i||^2]\\&+\sum_{j=1}^{n}\lambda_j\left(1-\sum_{i=1}^{c}u_{ij}\right).\end{aligned}\tag{16}$$

Taking the partial derivative of L with respect to u_{ij} and λ_j and setting them to zero, we obtain

$$\frac{\partial L}{\partial u_{ij}} = 0 \Leftrightarrow m u_{ij}^{m-1} ||x_j - v_i||^2 + a_j - m a_j u_{ij}^{m-1} + m\beta_j u_{ij}^{m-1} ||\bar{x}_j - v_i||^2 - \lambda_j = 0 \quad (17)$$

$$\frac{\partial L}{\partial \lambda_j} = 0 \Leftrightarrow 1 - \sum_{i=1}^{c} u_{ij} = 0. \quad (18)$$

From Eq. (17), we have

$$u_{ij} = \left(\frac{\lambda_j - a_j}{m(||x_j - v_i||^2 - a_j + \beta_j ||\bar{x}_j - v_i||^2)} \right)^{1/(m-1)}. \quad (19)$$

Substituting Eq. (19) into Eq. (18), we obtain

$$\left(\frac{\lambda_j - a_j}{m} \right)^{1/(m-1)} = \frac{1}{\sum_{l=1}^{c} (||x_j - v_l||^2 - a_j + \beta_j ||\bar{x}_j - v_l||^2)^{-1/(m-1)}}. \quad (20)$$

Substituting Eq. (20) into Eq. (19), thus we have

$$u_{ij} = \frac{1}{\sum_{l=1}^{c} \left(\frac{||x_j - v_i||^2 - a_j + \beta_j ||\bar{x}_j - v_i||^2}{||x_j - v_l||^2 - a_j + \beta_j ||\bar{x}_j - v_l||^2} \right)^{1/(m-1)}}. \quad (21)$$

Similarly, taking the partial derivative of L with respect to v_i and setting it to zero, we have

$$\frac{\partial L}{\partial v_i} = 0 \Leftrightarrow 2 \sum_{j=1}^{n} u_{ij}^m (x_j - v_i) + 2 \sum_{j=1}^{n} \beta_j u_{ij}^m (\bar{x}_j - v_i) = 0. \quad (22)$$

From Eq. (22), we obtain

$$v_i = \frac{\sum_{j=1}^{n} u_{ij}^m (x_j + \beta_j \bar{x}_j)}{\sum_{j=1}^{n} (1 + \beta_j) u_{ij}^m}. \quad (23)$$

This completes the proof. □

References

[1] N.R. Pal, S.K. Pal, A review on image segmentation techniques, Pattern Recognition 26 (9) (1993) 1277–1294.
[2] H. Zhou, Y. Yuan, F. Lin, T. Liu, Level set image segmentation with Bayesian analysis, Neurocomputing 71 (10–12) (2008) 1994–2000.
[3] T. Liu, H. Zhou, F. Lin, Y. Pang, J. Wu, Improving image segmentation by the gradient vector flow and mean shift, Pattern Recognition Lett. 29 (1) (2008) 90–95.
[4] Y. Jiang, Z.H. Zhou, SOM. ensemble-based image segmentation, Neural Process. Lett. 20 (3) (2004) 171–178.
[5] S.R. Kannan, A new segmentation system for brain MR images based on fuzzy techniques, Appl. Soft Comput. 8 (4) (2008) 1599–1606.
[6] X. Yang, W. Zhao, Y. Chen, X. Fang, Image segmentation with a fuzzy clustering algorithm based on Ant-Tree, Signal Process. 88 (10) (2008) 2453–2462.
[7] W. Hung, M. Yang, D. Chen, Bootstrapping approach to feature-weight selection in fuzzy *c*-means algorithms with an application in color image segmentation, Pattern Recognition Lett. 29 (9) (2008) 1317–1325.
[8] H. Zhou, G. Schaefer, A. Sadka, M.E. Celebi, Anisotropic mean shift based fuzzy *c*-means segmentation of dermoscopy images, IEEE J. Sel. Top. Signal Process. 3 (1) (2009) 26–34.
[9] J.C. Bezdek, Pattern Recognition with Fuzzy Objective Function Algorithms, Plenum, New York, 1981.
[10] J.L. Fan, W.Z. Zhen, W.X. Xie, Suppressed fuzzy *c*-means clustering algorithm, Pattern Recognition Lett. 24 (9–10) (2003) 1607–1612.
[11] L. Zhu, F.L. Chung, S.T. Wang, Generalized fuzzy *c*-means clustering algorithm with improved fuzzy partitions, IEEE Trans. Syst., Man, Cybern. B, Cybern. 39 (3) (2009) 578–591.
[12] M.N. Ahmed, S.M. Yamany, N. Mohamed, A.A. Farag, T. Moriarty, A modified fuzzy *c*-means algorithm for bias field estimation and segmentation of MRI data, IEEE Trans. Med. Imaging 21 (3) (2002) 193–199.
[13] S.C. Chen, D.Q. Zhang, Robust image segmentation using FCM with spatial constraints based on new kernel-induced distance measure, IEEE Trans. Syst., Man, Cybern. B, Cybern 34 (4) (2004) 1907–1916.
[14] K.S. Chuang, H.L. Tzeng, S. Chen, J. Wu, T.J. Chen, Fuzzy *c*-means clustering with spatial information for image segmentation, Comput. Med. Imaging Graphics 30 (1) (2006) 9–15.
[15] W.L. Cai, S.C. Chen, D.Q. Zhang, Fast and robust fuzzy *c*-means clustering algorithms incorporating local information for image segmentation, Pattern Recognition 40 (7) (2007) 825–838.
[16] A. Buades, B. Coll, J.M. Morel, A non-local algorithm for image denoising. in: Proc. IEEE Int. Conf. Comput. Vision Pattern Recognition. (2005) 60–65.
[17] M. Wu, B. Scholkopf, A local learning approach for clustering. in: Advances in Neural Information Processing Systems 19. (2007) 1529–1536.
[18] J.C. Bezdek, Cluster validity with fuzzy sets, Cybern. Syst. 3 (3) (1973) 58–73.
[19] J.C. Bezdek, Mathematical models for systematic and taxonomy. in: Proc. of eighth international conference on numerical taxonomy. (1975) 143–166.